catalysts

MDPI

Article

A Model of Catalytic Cracking: Catalyst Deactivation Induced by Feedstock and Process Variables

Galina Y. Nazarova *, Elena N. Ivashkina, Emiliya D. Ivanchina and Maria Y. Mezhova

Division for Chemical Engineering, National Research Tomsk Polytechnic University, 634050 Tomsk, Russia; ivashkinaen@tpu.ru (E.N.I.); ied@tpu.ru (E.D.I.); mym6@tpu.ru (M.Y.M.)
* Correspondence: silko@tpu.ru; Tel.: +7-(3822)-701-777 (ext. 1476)

Abstract: Changes in the quality of the feedstocks generated by involving various petroleum fractions in catalytic cracking significantly affect catalyst deactivation, which stems from coke formed on the catalyst surface. By conducting experimental studies on feedstocks and catalysts, as well as using industrial data, we studied how the content of saturates, aromatics and resins (SAR) in feedstock and the main process variables, including temperature, consumptions of the feedstock, catalyst and slops, influence the formation of catalytic coke. We also determined catalyst deactivation patterns using TG-DTA, N_2 adsorption and TPD, which were further used as a basis for a kinetic model of catalytic cracking. This model helps predict the changes in reactions rates caused by coke formation and, also, evaluates quantitatively how group characteristics of the feedstock, the catalyst-to-oil ratio and slop flow influence the coke content on the catalyst and the degree of catalyst deactivation. We defined that a total loss of acidity changes from 8.6 to 30.4 wt% for spent catalysts, and this depends on SAR content in feedstock and process variables. The results show that despite enriching the feedstock by saturates, the highest coke yields (4.6–5.2 wt%) may be produced due to the high content of resins (2.1–3.5 wt%).

Keywords: saturates; resins; aromatics; catalyst-to-oil ratio; slops; catalyst; coke; activity

Citation: Nazarova, G.Y.; Ivashkina, E.N.; Ivanchina, E.D.; Mezhova, M.Y. A Model of Catalytic Cracking: Catalyst Deactivation Induced by Feedstock and Process Variables. *Catalysts* **2022**, *12*, 98. https://doi.org/10.3390/catal12010098

Academic Editor: Changzhi Li

Received: 1 December 2021
Accepted: 10 January 2022
Published: 14 January 2022

1. Introduction

Currently, a tendency to produce heavier crude oil generates the need for improving advanced petroleum refining processes both through the development and application of high activity and selective forms of catalysts and the prediction and optimization of their operating variables using predictive models [1–3]. The main factors affecting catalyst properties include feedstock type, process variables and their acid and structural properties, particularly the size and volume of mesopores and micropores, surface area, strength and density of acid sites.

This poses a major challenge for scientists, i.e., how to develop a functional relationship among the hydrocarbon composition of feedstocks, the variables of deep oil refining processes, as well as catalyst activity taking into account the kinetic patterns of coke deposition on catalysts.

Modern catalysts are high-aluminous complex composite systems containing a wide porous aluminosilicate matrix and active component. The content of Al_2O_3 in catalysts is usually about 40–45 wt%. The active components, which are of industrial interest on catalytic cracking, are presented by zeolites in rare-earth or decationic forms, such as FAU (X, Y), BEA (BETA), MFI (ZSM-5), FER (Ferrierite), MOR (Mordenite), MWW (MCM-22), Z-21, Z-22, etc. Zeolites Y and ZSM-5 showed a high selectivity in relation to high yield of gasoline and light alkenes [4–6]. Mesoporous and macroporous structures facilitate the preliminary splitting of large heavy oil molecules in order to diffuse into the micropores of the Y-zeolite and are selectively cracked into the desired products.

Changes in feedstock quality generated by involving various petroleum fractions in catalytic cracking such as the content of saturates, aromatics and resins (SAR) affect significantly catalyst deactivation, which stems from the coke formed on the catalyst's surface [7]. The results [8] indicate that catalyst fouling decreases notably by incorporating polyolefins as a catalytic cracking feedstock, changing coke nature to a more aliphatic (olefinic) one and its location towards zeolite micropores. They showed that the coke formed from the vacuum gasoil is more evolved and mainly constituted by polyaromatic components deposited on the mesopores of the catalyst matrix, which affects product distribution.

In order to describe the catalyst deactivation of zeolite catalysts, scientists have successfully employed several approaches, such as Time-on-Stream [9–11] or Coke-on-Catalyst [12,13] theories, as well as selective description that considers the different catalyst deactivation effects on the reactions or reaction groups, affecting the products [14–16]. Other studies take into account catalyst deactivation by diffusion restrictions arising from pore clogging by coke using the effectiveness factor [17] or by a function of heavy aromatics adsorption formed from various reactions paths [18]. Special attention has been paid to the assessment of different types of coke deposited and their chemical nature (physical and chemical) on the basis of the experimental dependence of coke yield on catalyst-to-oil ratio [19]. Kinetic patterns of total amount of coke formed from heavy, light-cycle oil or naphtha were defined, which is in concordance with the well-established role of heavy aromatics in the formation of coke. However, such an approach fails to predict the feedstock effect on catalyst deactivation.

Although the coke-formation ability of feedstock can be indirectly estimated using density, coking capacity, K-factor and refractive index, the feedstock components resulting in coke formation include polycyclic arenes, resins and asphaltenes. Generally, hydrocarbons can be arranged in sequence, paraffinic <naphthenic <aromatic, whereas the amount of coke and the catalyst deactivation degree is significantly influenced by both the continuous change in the content of each hydrocarbons group and process variables, including catalyst-to-oil ratio, temperatures and feedstock and catalysts consumptions. Moreover, according to industrial data, some slops from separation column are passed to the middle part of the riser. This flow contains a high amount of polycyclic aromatic hydrocarbons, which significantly affects coke formation. The coke deactivating effect on USHY zeolite increases with increasing contact time [20]. At high values of contact time, the blocking of the active surface, the inlet pores and channels in the zeolite may occur. Such conditions result in the formation of graphitized coke and irreversible deactivation by the pore clogging. In [21], the authors describe the effect of the catalyst-to-oil ratio on activity of three FCC catalysts using 1,3,5-tri-isopropyl benzene experimentally. They show that catalyst density affects both catalyst coking and deactivation, displaying an optimum catalyst-to-oil ratio for achieving maximum hydrocarbon conversions in FCC units.

Moreover, the SAR content and catalyst-to-oil ratio can vary over a wide range resulting in a decrease or increase in catalyst deactivation continuously. Herewith, the formation and accumulation of coke and its structure depend significantly on the type and chemical composition of the catalysts [22]. Therefore, in order to quantify the influence of SAR content in feedstock on coke formation, a kinetic model of the catalytic cracking is required, which should be sensitive to hydrocarbon groups. Such models should take into account the change in SAR content in the feedstock, the kinetic parameters of the high molecular hydrocarbon conversion, the process variables and the properties and deactivation constant of the catalyst from the unit under study.

In this paper, we study how SAR content in the catalytic cracking feedstock and the main process variables, including the feedstock, catalyst and slops temperatures and consumptions, influence the formation of catalytic coke. The latter forms on the catalyst's surface when the reactions of cyclization, aromatization, hydrogen transfer and condensation occur in a riser. We also discussed how this coke affects catalyst properties and deactivation patterns, which were further used as a basis for a kinetic model of catalytic cracking. This model helps predict the changes in reactions rates caused by coke forma-

tion and, also, evaluates quantitatively how group characteristics of the feedstock, the catalyst-to-oil ratio and slop flows influence coke content on the catalyst and the degree of catalyst deactivation.

2. Results and Discussion

2.1. Experimental

2.1.1. Feedstocks

In order to evaluate how feedstock properties affect coke formation, we defined experimentally the SAR content, density and molecular weight of various catalytic cracking feedstocks on the unit under study (Table 1).

Table 1. Results of laboratory study of catalytic cracking feedstocks.

Properties and Groups	Feeds						
	#1	**#2**	**#3**	**#4**	**#5**	**#6**	**#7**
IBP, °C	301.0	304.0	303.0	304.0	316.0	317.0	318.0
10%, °C	346.0	347.0	3430.	347.0	346.0	354.5	372.0
50%, °C	411.0	413.5	413.0	413.5	412.0	421.0	433.0
90%, °C	494.0	492.0	492.0	491.0	491.0	492.5	497.0
FBP, °C	541.0	5410.	537.0	541.5	539.0	541.0	542.0
Density 20 °C, kg/m^3	888.0	886.0	888.0	888.0	892.0	890.0	893.0
Molecular weight, g/mol	331.3	330.3	343.3	339.7	345.1	338.5	342.2
Saturates, wt%	68.2	67.4	59.6	65.3	57.7	67.7	67.3
Aromatics, wt%	30.2	30.5	38.5	32.0	39.2	29.4	29.2
Resins, wt%	1.6	2.1	1.9	2.9	3.0	2.9	3.5

The results demonstrated that feedstock properties differ significantly. The boiling point of 50% changes from 409.5 to 433.0 °C. Although the densities of these feeds are closed, SAR content varies in a wide range. The content of saturates changes from 59.6 to 68.2 wt%, and the amount of aromatics and resins varies from 29.4 to 39.2 wt% and from 1.6 to 3.5 wt%, which influenced process efficiency and the degree of coke formation.

According to Table 1, we separate these feedstocks into four groups: saturated (feeds #1 and #2), aromatic (feed #3), aromatic and resinous (feed #5), as well as saturated and resinous (feeds #4, #6 and #7). Taking into account that catalytic cracking feedstocks change continuously, this helps in the evaluation of how feedstock composition influences the rate of coke formation and, further, catalyst deactivation.

2.1.2. Catalysts

By overall studying cracking catalysts, we defined how coke content on the catalyst surface impacts the catalyst deactivation. Figure 1 shows thermogravimetric results of spent catalysts when Feed #1 and Feed #6 were converted. Since temperatures of coke oxidation were detected at a temperature less than 740 °C for both samples, the coke had an amorphous structure for each feed and process variable. Nevertheless, the temperatures of coke oxidation exothermic peak differ significantly (510 and 563 °C), which indicates that coke from saturated feed is more enriched by hydrogen.

The presence of amorphous coke was also confirmed by a thermogram of the spent catalyst with a charge–mass distribution z/m = 44 (Figure 1b). In this case, an ion current peak appeared at a temperature range of 465–650 °C. This indicates the presence of CO_2 gas formed during the oxidation of the amorphous coke. The total weight of the catalysts reduced by 0.98 and 1.4 wt% for Feed#1 and Feed#6 when catalysts were heated up to 700 °C.

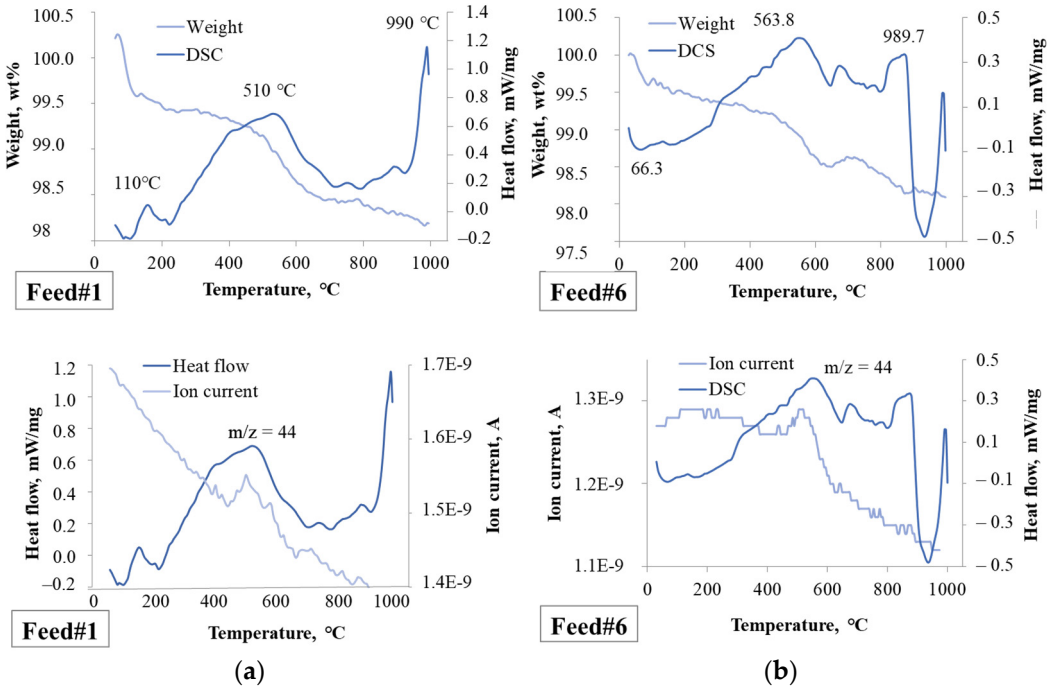

Figure 1. Thermogravimetric results with charge-mass distribution: (**a**) Thermogram for spent catalysts when Feed#1 is converted; (**b**) Thermogram for spent catalysts when Feed#6 is converted.

Table 2 presents the change in surface area, volume and size of mizopores and micropores of spent and regenerated catalysts.

Table 2. Results of laboratory study of catalytic cracking catalysts.

Properties	Catalyst	
	Regenerated	**Spent**
BET surface area, m^2/g	133.2–141.1	122.6–131.8
Pore volume, mm^3/g	157.0–179.0	150.0–152.0
BJH method (pore size is 1.7–300 nm)		
Surface area of pore, m^2/g	31.4–38.4	27.3–31.3
Pore volume, mm^3/g	113.0–139.0	108.0–130.0
Average pore size, nm	14.8–17.8	13.8–14.4
De Boer t-method		
Micropore surface area, m^2/g	110.9–115.9	104.2–101.2
Micropore volume, mm^3/g	56.0–60.0	53.0–56.0
Horvath–Kawazoe		
Maximum pore volume, mm^3/g	67.0–69.0	63.0–65.0
Median pore width, Å	7.1–7.2	7.0–7.1

We detected IV type of adsorption isotherm; a steep region is observed in the area of low relative pressure, which is related to a high adsorption potential and indicates the presence of micropores and capillary condensation in mesopores. This type of hysteresis loop is, normally, observed in materials with slit pores. The results showed that the catalyst have a high micropore surface area (110.9–115.9 m^2/g), which facilitates the selective cracking of low molecular weight hydrocarbons to form light olefins. The decrease in the specific surface area from regenerated to spent catalysts was 3.1–10.2 wt%, and the change in the total pore volume reaches 14.9%. The decrease in the surface area and the volume of mesopores and micropores achieved 23.5 and 20.1%, as well as 10.1 and 10.2%, respectively. The size of micropores before and after regeneration changes insignificantly by 0.72–2.5%, and the change in the size of mesopores reaches 3.0–22.2%.

Another important characteristic of catalysts, which affects their activity, is acid properties [23]. The results of TPD showed that subacid sites attend the catalysts due to the presence of one form of desorption of ammonia on the thermal desorption spectrum. The temperatures of peak maximum are equal to 95–140 °C and 100–125 °C for regenerated and spent catalysts [24], and the total amount of desorbed ammonia decreases from regenerated to spent catalysts. Moreover, the specific surface area correlates with the total number of acid sites on regenerated samples, for catalyst #4 these values are 141.1 m^2/g and 232 μmol/g. The number of acid sites varies in the range of 216–232 μmol/g. The total loss in acidity of the coked catalysts relative to regenerated samples was 8.6–30.4 wt%. Furthermore, these results will be compared with the coke content on the cracking catalyst and other factors of catalytic cracking in order to take into account catalyst deactivation during modeling.

2.2. Modelling

Figure 2 illustrated an approach for accounting for catalyst deactivation when the mathematical model of catalytic cracking was developed. In order to define catalyst deactivation patterns, we combined the experimental study of feedstock and catalysts with industrial data from the catalytic cracking unit, including the coke amount and process variables.

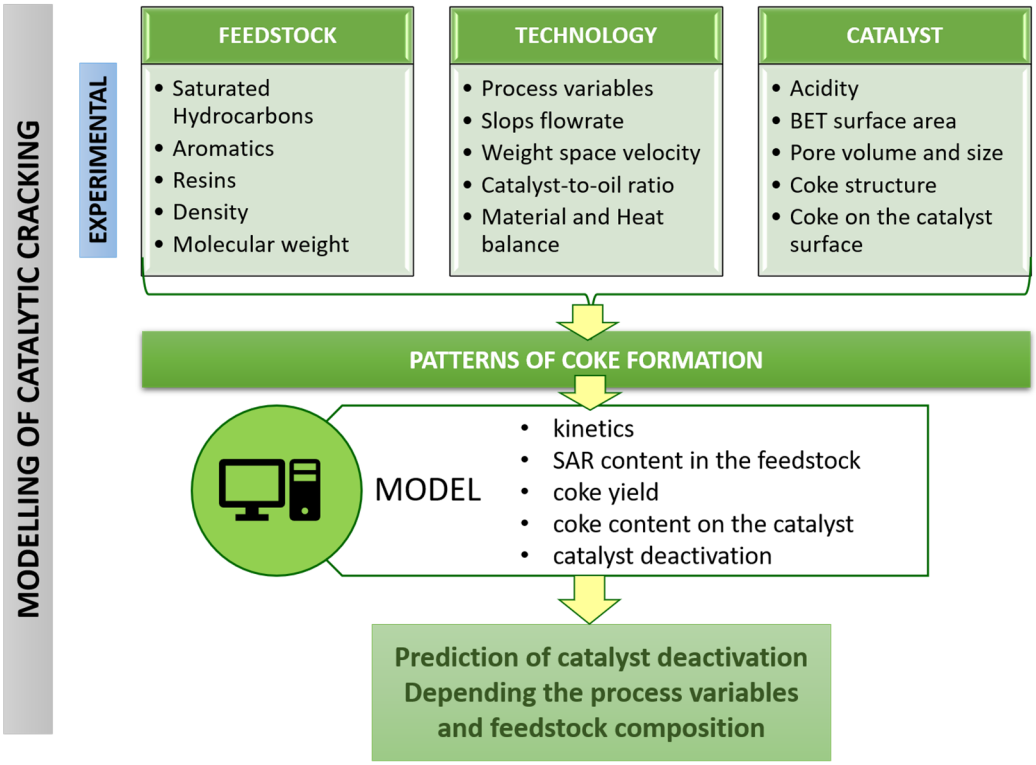

Figure 2. An approach for accounting for catalyst deactivation during modeling.

2.2.1. Effect of the Feedstock Composition and Process Variables on Coke Formation

A change in main operating variables of the riser for each feedstock is shown in Table 3.

Table 3. Operating variables of the catalytic cracking riser (industrial data).

Process Conditions	Feed						
	#1	#2	#3	#4	#5	#6	#7
Weight space velocity, kg/(kg·h)	0.14	0.13	0.13	0.12	0.14	0.11	0.11
Feedstock temperature, °C	295.80	283.90	294.00	291.80	306.10	288.20	302.50
Slops flow rate to reactor, m^3/h	10.00	10.70	9.40	13.30	11.10	18.90	19.10
Water vapor flow to reactor gripper, tons/h	5.50	5.50	5.50	5.50	5.50	6.10	6.90
Water vapor consumption for spraying feedstocks, kg/h	2400.00	2400	2400.00	2400.00	2400.00	2400.00	2400.00
Regenerated catalyst temperature, °C	665.40	662.80	664.50	660.66	662.30	660.70	661.50
Pressure in the reactor, MPa	1.56	1.53	1.52	1.36	1.43	1.39	1.24
Catalyst/oil ratio, $tons_{cat}/tons_{feedstock}$	7.40	7.80	7.70	8.10	7.40	9.27	9.20

The yield and content of coke on the catalyst vary from 3.7 to 5.7 wt% and from 0.48 to 0.63 wt%, respectively (Figure 3). When we studied how SAR content in the feedstock influences coke yield and catalyst deactivation, the parameters of catalyst-to-oil ratio, slops flowrate, temperature and weight space velocity were equal due to their significant influences on coke formation in riser. We found that, for saturated-resinous feedstocks (Feed #6 and #7), the coke yield increases by 0.3wt% when the content of resins changes from 2.9 to 3.5 wt%. A similar pattern was observed for aromatics and resinous feedstocks (Feeds # 1 and # 5); the coke yield is higher by 0.4% wt. for feedstock #5, when slop consumption for the latter is also slightly higher by 1.1 m^3/h. Although Feed #3 contains a higher content of aromatics compared to feed #2, the coke yield (3.7 wt%) was lower, which stems from both a lower slop flowrate to riser and low content of resins (by 0.2 wt%) in feed.

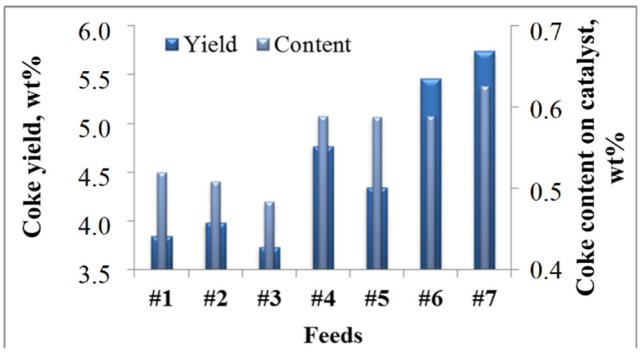

Figure 3. Coke yield and content depending on the SAR amount in feedstock (industrial data).

Moreover, the coke content on the catalyst and its structure depend significantly on catalyst operating variables. An increase in catalyst-to-oil ratio promotes both rising the cracking temperature and reduces coke content on the catalyst's surface, which contributes to an increase in average catalyst activity at the riser's outlet. Such patterns are observed for Feeds #4–6 when the coke yields differ significantly, while the coke contents on the catalyst were at a constant level (0.59 wt%). This stems from increasing the catalyst-to-oil-ratio and their effects on catalyst deactivation. Despite an increasing coke yield, its content decreases, resulting in a rise of average catalyst activity. Since the contact time between feedstock and catalyst is around 4.7–5.03 s, which is relatively low, we can only assume that the catalyst is deactivated to a greater extent by the poisoning of acid sites [25].

These results confirmed that both the catalyst operation in the riser and SAR content in the feedstock significantly affect coke formation, especially when the higher resinous and arenas feedstocks are converted. For this reason, the deactivation effect can differ considerable depending on these factors. Furthermore, we studied how the coke content on the catalyst influences catalyst deactivation under industrial operating variables.

2.2.2. Patterns of Catalyst Deactivation by Coke

The most important properties of a catalyst include both the characteristics of acid sites (strength and density) and textural properties such us pore structure, sizes and shapes of cavities and channel intersections, etc. For heterogeneous catalysis, catalyst activity depends on the number and nature of active sites involved in the catalytic process. Activity of the catalyst can be proportional to the surface value where the active centers are located. For example, for porous catalysts, only the surface accessible to the reagents is active. In a first approximation to assess the change in catalyst activity, we used the specific surface area (Figure 4), which, generally, correlates with the coke content on the catalyst. The greatest change from 6.0 to 10.6% was observed for saturated and resinous feedstock, while an increase in the catalyst-to-oil ratio decreases the content of coke on the catalyst and increases the total specific surface area of the catalyst.

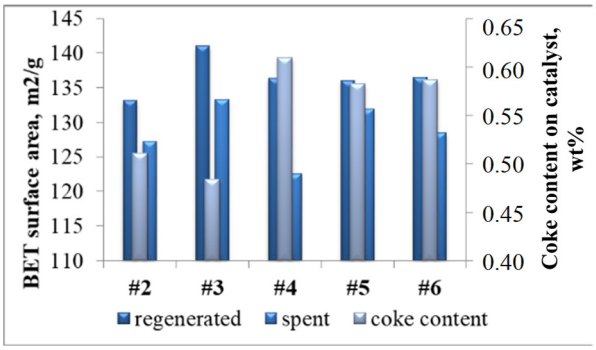

Figure 4. Change in specific surface area and coke content on the catalysts.

According to [26], the initial rate of coke formation correlates with the density of acid sites, while the selectivity to coke formation depends on the pore's size [27]. TPD results allowed us to determine the dependence of total amount of desorbed ammonia from the catalyst on the content of coke on the catalyst (Figure 5). The results shows that although the concentrations of the acid sites for regenerated catalysts #2 and #6 were lower (216–224 μmol/g) compared catalyst #4 (232 μmol/g), the decrease in total acidity of spent catalyst #2 and #6 was the greatest by 1.3–1.4, which correlates with coke content on the catalyst.

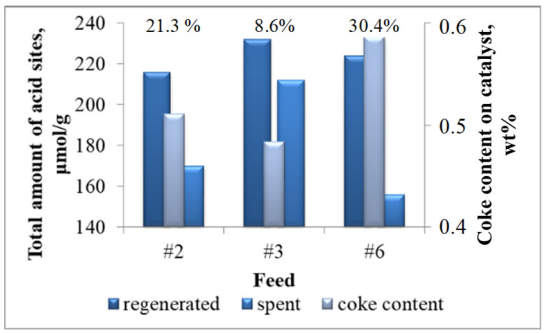

Figure 5. Dependence of total amount of desorbed ammonia from the catalyst surface on the content of coke on the catalyst.

Despite containing a large amount of aromatics in Feed #4, the content of coke on the catalyst is significant lower in comparison to Feed #2, which is caused by lower deactivation and an increase in average catalyst activity. This stems from the high amount of slop flow relative to the riser (9.35 m^3/h), as well as higher contents of resins in Feed #2. TPD results were compared with coke content on spent and regenerated catalysts. We determined that the total acidity loss for catalyst increased from 8.6 to 30.4 wt% when coke content

on the catalyst increased from 0.48 to 0.59 wt%. The coke content on the regenerated catalyst was 0.02–0.06 wt%. Figure 6 presents the dependence of acidity change when coke content on the catalyst changes from 0 to 0.61 wt%. By using experimental data, we defined the value of catalyst deactivation constant for this catalyst, which was equal to 0.729. These patterns are in concordance with [28], when demonstrated that the number of coke molecules causing complete deactivation (2.4 and 1.7, respectively) is close to the number of strong acid sites (1.6 and 3.4 for ZSM-5 and Y). In addition, the lower hydrogen transfer rate for HZSM5 as compared to HY is explained either by the smaller size of the available space near acid sites (8.5 and 13 Å for HZSM5 and HY) or by 10 times lower its density [27]. These patterns served as the basis of the catalytic cracking kinetic model, taking into account coke formation and kinetic parameters of catalytic cracking reactions, which involves high-molecular hydrocarbons.

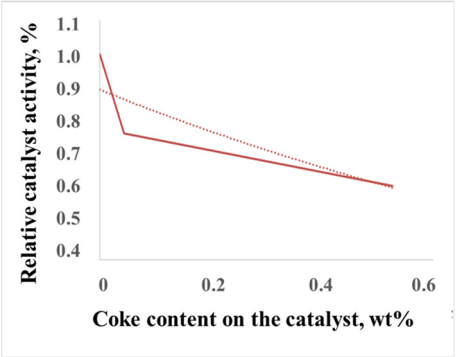

Figure 6. Dependence of relative catalyst activity on the coke content on the catalyst.

2.2.3. The Model

Previous comprehensive experimental studies allow us to form a reaction network of catalytic cracking [29–31]. The formalized mechanism of cracking reactions simplifies the mathematical description of such complicated multicomponent processes and considers SAR composition and reactions resulting in coke formation from these hydrocarbons. Therefore, this mechanism allows us to predict the amount of coke as well as the catalyst's deactivation degree.

We used the SAR content in the feedstock, the process conditions such as weight space velocity, the temperatures of feedstock, catalyst and slop flowrate relative to the riser as input data to the model. The mathematical model (Equation (1)) represents a system of ordinary differential equations describing material and heat balances. The riser is modeled as a plug flow reactor, for gas velocity (~3.2–9.2 m/s) significantly exceeds the initial fluidizing velocity and the Peclet diffusion number tends to infinity.

$$\begin{cases} \frac{dC_i}{d\tau} = \sum\limits_{j=1}^{18} (\pm\psi \cdot (\overrightarrow{W} - \overleftarrow{W})_j) \\ p_m c_m \frac{dT}{d\tau} = \sum\limits_{j=1}^{18} (\pm\psi \cdot ((\Delta_r \overrightarrow{H_T^\circ}) \cdot \overrightarrow{W})_j - ((\Delta_r \overleftarrow{H_T^\circ}) \cdot \overleftarrow{W})_j)) \end{cases} \quad (1)$$

Initial conditions: $C_i = C_{i0}$, $T_0 = T_{it}$. Here, C_i is the concentration of i-the hydrocarbons group, mol/m^3; τ is the contact time, s; i and j are the component and reaction numbers; ψ is the deactivation function (3); $\overrightarrow{W}$ and $\overleftarrow{W}$ are the reaction rates in the forward and reverse directions, mol/(s·m^3); p_m and c_m are the density and heat capacity of flow, kg/m^3, kJ/kg K; T is the temperature; $\Delta r\overrightarrow{H_T^\circ}$ and $\Delta r\overleftarrow{H_T^\circ}$ are the thermal effects of the chemical reactions, kJ/mol; and T_{it} is the initial temperature of cracking, K.

The interdependence between reaction rates (18 reactions) and group concentrations (14 components) is based on the law of mass action according to reaction network (Figure 2).

Moreover, the reaction rate is multiplied by the catalyst deactivation parameter, calculating component concentrations (Equation (2)).

$$W_j = \psi \cdot k_j \cdot C_i \quad (2)$$

In order to provide a mathematical description of reversible catalyst deactivation by coke, we used the Coke-on-Catalyst approach. The catalyst deactivation parameter ψ is calculated depending on the coke content on its surface. Using the results of TPD, we defined the dependence of acid properties of the catalyst on coke concentration (Equation (3)).

$$\psi = f(C_k) = A = A_0 \cdot e^{-0.729 \cdot C_{coke}} \quad (3)$$

Here, A is the current relative catalyst activity (acidity), %; A_0 is regenerated catalyst activity, %; and C_{coke} is the coke content on the catalyst, wt%.

This approach allows us to implement the relationship among the following parameters: the composition of the feedstock; the content of coke on the catalyst; the change in catalyst activity; and the change in the yield and composition of the products. Table 4 presents estimated kinetic parameters of the reactions when high molecular weight hydrocarbons were converted into gas, gasoline, diesel fractions and coke.

Table 4. The kinetic patterns of catalytic cracking.

No.	Reaction	k_{801}, s^{-1} or $L \cdot s^{-1}$ mol^{-1}
1	C_{13}–C_{40}Alkanes ↔ C_5–C_{12}Alkanes + C_5–C_{12}Unsaturated HC	0.10
2	C_{13}–C_{40}Alkanes ↔ C_5–C_{12}Isoalkanes + C_5–C_{12}Unsaturated HC	0.53
3	HMW Cycloalkanes ↔ C_5–C_{10} Cycloalkanes + 2 C_5–C_{12}Unsaturated HC	0.10
4	HMW Aromatics ↔ C_5–C_{12} Aromatics + 2 C_5–C_{12}Unsaturated HC	0.31
5	HMW Cycloalkanes ↔ C_5–C_{12} Aromatics + $2H_2$ + PPF	0.31
6	C5–C12 N-alkanes ↔ PPF + BBF	0.02
7	C5–C12 Isoalkanes ↔ PPF + BBF	0.02
8	C5–C12Unsaturated HC ↔ 2 Gas	0.11
9	C_5–C_{12} Unsaturated HC ↔ BBF + BBF	0.15
10	C_5–C_{12} Unsaturated HC ↔ PPF + PPF	0.09
11	C_6–C_{12} Aromatics ↔ C_6–C_{12} Aromatics + C_5–C_{12} Unsaturated HC	0.13
12	C_5–C_{12} Unsaturated HC C_5–C_{10} ↔ C_5–C_{10} Cycloalkanes	0.05
13	C_5–C_{12} Unsaturated HC + PPF ↔ C_5–C_{12} Aromatics + $2H_2$	0.34
14	2 C_5–C_{12}Unsaturated HC ↔ C_5–C_{10} Cycloalkanes + C_5–C_{12}Isoalkanes 2	8.90
15	C_5–C_{12}Unsaturated HC + C_5–C_{10} Cycloalkanes ↔ C_5–C_{12} Aromatics + C_5–C_{12}Isoalkanes	31.5
16	C_6–C_{12} Aromatics + C_5–C_{12}Unsaturated HC ↔ HMW Aromatics + $2H_2$	0.21
17	HMW Aromatics + C_6–C_{12} Aromatics ↔ CNAC + $2H_2$	0.77
18	CNAC ↔ COKE + $3H_2$	0.48

The mathematical model was verified by comparing the calculated data of the coke yields and catalyst coke content with industrial data (Figure 7). A change in main operating variables of the riser is presented in Table 3, and feedstock composition changed according to Table 1.

A verification of the model shows that the average relative error between calculated and experimental data is less than 7.0 wt%.

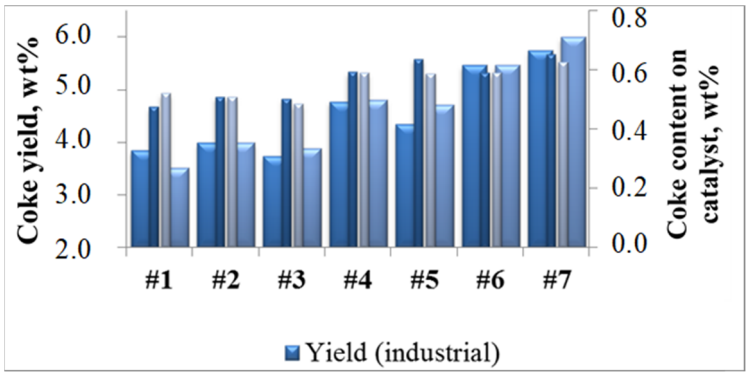

Figure 7. Comparison between model and experimental results by yields and content of coke on catalysts.

2.2.4. Application of Model

The use of the model helps in quantitatively evaluating how each discussed parameter influenced the yield and coke content on the catalyst, as well as the degree of catalyst deactivation.

Figure 8 shows the effect of different feedstocks (Table 1) on coke yields, its content on the catalyst and the relative catalyst activity when the operating variables were equal to #2 (Table 3). Model-based calculations presented a conversion of saturated feeds (Feed #1 and #2) that ensure the smallest amount of coke (3.5–3.9% mac.); on the other hand, despite containing a high amount saturates in Feeds #4, #6 and #7, they produce the highest coke yields (4.6–5.2 wt%). When the resin's content in the catalytic cracking feedstock increased from 1.9 to 3.0 wt%. in aromatic feeds (Feed #3 and #5), coke yields increased by 1.0 wt%. Increasing the slop flow to riser by 15 m^3/h also increases coke yield by 0.64–0.68 wt% for Feeds #2 and #7, which results in increased catalyst deactivation (Figure 9). Generally, an increase in catalyst coke content reduced relative catalyst activity by 12.3%.

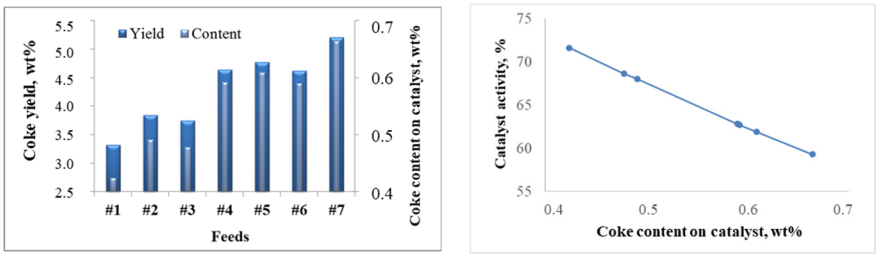

Figure 8. Feedstock-induced changes in coke yield, its content on the catalyst and relative catalyst activity.

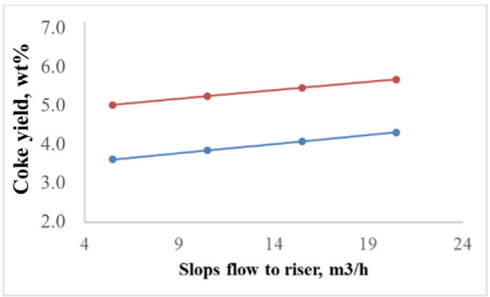

Figure 9. Effect of the slop flowrate relative to riser on coke yield.

Figures 10 and 11 show how the catalyst-to-oil ratio influences coke yield and its content on the catalyst, as well as the relative catalyst activity. When the catalyst-to-oil ratio increased from 5.0 to 10.5 $tons_{cat}/tons_{feed}$, coke yield increases from 2.4 to 5.5 wt%

for Feeds #2 and from 3.2 to 6.0 wt% for Feeds #7, whereas the content of coke on the catalyst reduces up to 0.52–0.57 wt%, resulting in an increase in average catalyst activity by 5.8–7.1%. Since feedstock composition and catalyst-to oil ratio significantly affect heat balance, these results will be further used to optimize process variables in order to increase desired products and to retain catalyst resources.

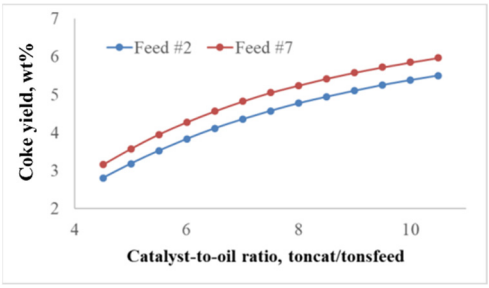

Figure 10. Effect of the catalyst-to-oil ratio on coke yield.

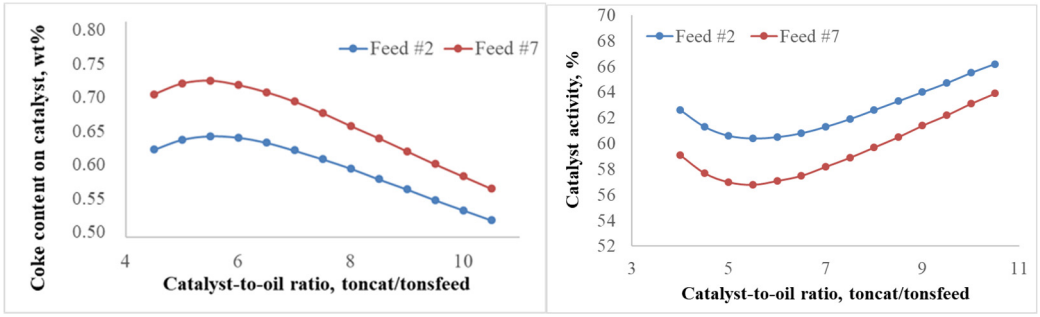

Figure 11. Effect of the catalyst-to-oil ratio on coke content and relative catalyst activity.

3. Methods

In our research, we studied a typical vacuum gasoil catalytic cracking unit with the circulated catalyst. We applied both the strategy of system analysis and experimental methods to study feedstock and catalyst properties.

The SAR content in the catalytic cracking feedstock was determined by liquid adsorption chromatography with gradient displacement using Gradient equipment. ASKG silica gel with grain size of less than 100 μ and mixed eluents were used as fixed and mobile phases.

After that, we conducted an experimental study on spent and regenerated catalysts, which facilitated the development of a model that also takes into consideration catalyst deactivation. The acid properties of both catalysts were studied by the method of temperature-programmed desorption of ammonia (TPD). Ammonia was adsorbed at 100 °C on a pre-trained sample and further desorbed from the zeolite surface in a linear heating mode at a rate of 10 K/min. The strength of the catalyst acid sites was estimated by the temperature maxima on the thermal desorption curve. The concentration of the acid sites was expressed in micromole (μmol) per 1 g of the catalyst and determined by the amount of ammonia desorbed when fixing desorption peaks. The textural properties of the catalysts were studied by nitrogen adsorption at −196 °C; using an automatic gas analyzer "TriStar 3020." The specific surface area of catalysts was determined by the BET method; the total volume of adsorption pores was measured at P/P0 = 0.99. The samples were preliminarily calcined at 350 °C for 2 h. Pore volumes in the range of 1.7–300 nm were defined by the BJH method on desorption branch, and the maximum volume and average size of micropores were calculated by using the Horvath–Kawazoe method. The quantity and structure of the coke on spent and regenerated catalysts were determined experimentally by the TG-DSC method (thermogravimetric analysis and differential-scanning calorimetry) using NETZSCH STA 449 F3. This equipment captured gravimetric analysis and registered

mass changes and thermal effects that occurred by changing the temperature and time of heating. The catalysts were heated from 50 to 1000 °C at a rate of 10 degrees C/min in corundum crucibles in the air.

Furthermore, we combined the experimental study of feedstock and catalysts with industrial data from the catalytic cracking unit such as coke amount and process variables. This helps in the evaluation of how SAR content in the feedstock and major process variables, including temperature, consumption of the feedstock, catalyst and slops, influence the formation of catalytic coke and the degree of the catalyst deactivation.

The above complex of experimental studies allowed us to upgrade the catalytic cracking model [32], which takes into consideration kinetic and catalyst deactivation patterns of catalytic cracking. By using the mathematical model, we predicted how the SAR content in feedstock, the slop's flow rate and the catalyst-to-oil ratio affect coke formation; moreover, we discussed how coke affects catalyst properties and deactivation.

4. Conclusions

Changes in the quality of the feedstocks generated by involving the various petroleum fractions in catalytic cracking significantly affect catalyst deactivation, which stems from coke formed on the catalyst's surface. The degree of catalyst deactivation depends on the operating variables and SAR content in the feedstock. A combination of the experimental study of feedstock and catalysts and industrial data from the catalytic cracking unit allowed us to study catalyst deactivation patterns by coke.

We developed a kinetic model for catalytic cracking, which ensures its sensitivity to SAR content in the feedstock and predicts how both each hydrocarbons types and the main process variables, including the catalyst-to-oil ratio and slop flow to riser, influence coke formation. Such a model helps predict a change in the reaction rate by coke at each calculation step and evaluates quantitatively how each discussed parameter influences the degree of catalyst deactivation.

The results showed that both the catalyst operation in the riser and SAR content in the feedstock significantly affect coke formation, especially when higher resinous and feedstock arenas are converted. Thus, despite enriching the feedstock by saturates, the highest coke yields (4.6–5.2 wt%) may be produced due to a high content of resins (2.1–3.5 wt%). We determined that the total loss of acidity for spent catalyst changes from 8.6 to 30.4 wt% depends on SAR content in feedstock and process variables. An increase in coke content on the catalyst reduces relative catalyst activity by 12.3%. When the catalyst-to-oil ratio rises from 5.0 to 10.5 $tons_{cat}/tons_{feed}$, coke yield increases from 2.4 to 5.5 wt% for feeds #2 and from 3.2 to 6.0 wt% for feeds #7, whereas the content of coke on the catalyst reduces up to 0.52–0.57 wt%, resulting in an increase in average catalyst activity by 5.8–7.1%. These results will further facilitate in optimizing feedstock composition and the heat balance of the process in order to increase desirable products and retain catalyst resources.

Author Contributions: Conceptualization, E.D.I.; funding acquisition, E.N.I.; investigation, G.Y.N.; methodology, E.D.I.; project administration, E.N.I.; resources, E.N.I.; software, G.Y.N.; supervision, E.N.I.; validation, M.Y.M.; visualization, G.Y.N. and M.Y.M.; writing—original draft, G.Y.N.; writing—review and editing, E.N.I. All authors have read and agreed to the published version of the manuscript.

Funding: This research was supported by TPU development program and Russian Foundation for Basic Research No. 21-53-10004.

Data Availability Statement: Not Applicable.

Acknowledgments: This research was supported by TPU development program and Russian Foundation for Basic Research No. 21-53-10004.

Conflicts of Interest: The authors declare no conflict of interest.

Abbreviations

SAR	saturates, aromatics and resins
PPF	propane–propylene fractions
BBF	butane–butylene fractions
k	reaction rate constant, s^{-1} or $L \cdot s^{-1}$ mol^{-1}
kn	the average number of naphthenic rings
m/z	mass-to-charge ratio
C_i	concentration of the i-th hydrocarbons group, mol/m^3
C_{i0}	initial concentration of the i-th hydrocarbons group, mol/m^3
T_0	initial temperature of cracking, K
T_{it}	the temperature of the thermal equilibrium between the feedstock and the catalyst, K
ΔrH°_{T}, ΔrH°_{T}	the thermal effects of the chemical reactions, kJ/mol
$\vec{W}$, $\overleftarrow{W}$	the reaction rate in the forward and reverse directions, $mol/(s \cdot m^3)$
T	temperature
p_m	the density of flow, kg/m^3
c_m	the heat capacity of flow, kJ/kg K
ψ	the deactivation function
j	the reaction number
τ	the contact time, s
i	number of components
j	number of reactions
A	the current relative catalyst activity (acidity), %
A_0	the regenerated catalyst activity, %
C_{coke}	the coke content on the catalyst, wt%

References

1. Belinskaya, N.S.; Lutsenko, A.S.; Mauzhigunova, E.N.; Afanaseva, D.A.; Ivanchina, E.D.; Ivashkina, E.N. Development of the approach to the modeling of the destructive catalytic hydroprocesses of atmospheric and vacuum distillates conversion. The case of oil distillates hydrodewaxing process. *Catal. Today* **2021**, *378*, 219–230. [CrossRef]
2. Yang, F.; Dai, C.; Tang, J.; Xuan, J.; Cao, J. A hybrid deep learning and mechanistic kinetics model for the prediction of fluid catalytic cracking performance. *Chem. Eng. Res. Des.* **2020**, *155*, 202–210. [CrossRef]
3. Zhang, Y.; Liu, M.; Zhao, L.; Liu, S.; Gao, J.; Xu, C.; Ma, M.; Meng, Q. Modeling, simulation, and optimization for producing ultra-low sulfur and high-octane number gasoline by separation and conversion of fluid catalytic cracking naphtha. *Fuel* **2021**, *299*, 120740. [CrossRef]
4. Sadrameli, S.M. Thermal/catalytic cracking of liquid hydrocarbons for the production of olefins: A state-of-the-art review II: Catalytic cracking review. *Fuel* **2016**, *173*, 285–297. [CrossRef]
5. Parthasarathi, R.S.; Alabduljabbar, S.S. HS-FCC High-severity fluidized catalytic cracking: A newcomer to the FCC family. *Appl. Petrochem. Res.* **2014**, *4*, 441–444. [CrossRef]
6. Castañeda, L.C.; Muñoz, A.D.; Ancheyta, J. Combined process schemes for upgrading of heavy petroleum. *Fuel* **2012**, *100*, 110–127. [CrossRef]
7. Bai, P.; Etim, U.J.; Yan, Z.; Mintova, S.; Zhang, Z.; Zhong, Z.; Gao, X. Fluid catalytic cracking technology: Current status and recent discoveries on catalyst contamination. *Catal. Rev.* **2019**, *61*, 333–4053. [CrossRef]
8. Rodríguez, E.; Elordi, G.; Valecillos, J.; Izaddoust, S.; Bilbao, J.; Arandes, J.M.; Castaño, P. Coke deposition and product distribution in the co-cracking of waste polyolefin derived streams and vacuum gas oil under FCC unit conditions. *Fuel Process. Technol.* **2019**, *192*, 130–139. [CrossRef]
9. Afshar Ebrahimi, A.; Mousavi, H.; Bayesteh, H.; Towfighi, J. Nine-lumped kinetic model for VGO catalytic cracking; using catalyst deactivation. *Fuel* **2018**, *231*, 118–125. [CrossRef]
10. Xiaojing, Z.; Shiyuan, S. Lumped Kinetic Modeling Method for Fluid Catalytic Cracking. *Chem. Eng. Technol.* **2020**, *43*, 2493–2500.
11. Elizalde, I.; Ancheyta, J. Modeling catalyst deactivation during hydrocracking of atmospheric residue by using the continuous kinetic lumping model. *Fuel Process. Technol.* **2014**, *123*, 114–121. [CrossRef]
12. Jarullah, A.T.; Awad, N.A.; Mujtaba, I.M. Optimal design and operation of an industrial fluidized catalytic cracking reactor. *Fuel* **2017**, *206*, 657–674. [CrossRef]
13. Moustafa, T.M.; Corella, J.; Froment, G.F. Kinetic modeling of coke formation and deactivation in the catalytic cracking of vacuum gas oil. *Ind. Eng. Chem. Res.* **2003**, *42*, 14–25. [CrossRef]
14. Jiménez-García, G.; Quintana-Solórzano, R.; Maya-Yescas, R. Improving accuracy in the estimation of kinetic frequency factors from laboratory data to model industrial catalytic cracking risers. *Ind. Eng. Chem. Res.* **2011**, *50*, 2736–2745. [CrossRef]

15. Fernandes, J.L.; Domingues, L.H.; Pinheiro, C.I.C.; Oliveira, N.M.C.; Ribeiro, F.R. Influence of different catalyst deactivation models in a validated simulator of an industrial UOP FCC unit with high-efficiency regenerator. *Fuel* **2012**, *97*, 97–108. [CrossRef]
16. Corella, J. On the Modeling of the Kinetics of the Selective Deactivation of Catalysts. Application to the Fluidized Catalytic cracking Process. *Ind. Eng. Chem. Res.* **2004**, *43*, 4080–4086. [CrossRef]
17. Jiménez-García, G.; Quintana-Solórzano, G.; Aguilar-López, R.; Maya-Yescas, R. Modelling Catalyst Deactivation by External Coke Deposition during Fluid Catalytic Cracking. *Int. J. Chem. Reactor Eng.* **2010**, *8*, e17027. [CrossRef]
18. Chen, Z.; Feng, S.; Zhang, L.; Wang, G.; Shi, Q.; Xu, Z.; Zhao, S.; Xu, C. Molecular-Level Kinetic Modeling of Heavy Oil FCC Process based on Hybrid Structural Unit and Bond-Electron Matrix. *AIChE J.* **2021**, 1–15. [CrossRef]
19. Roberto, P.; Rodríguez, E.; Gutierrez, A.; Bilbao, J.; Arandes, J. Kinetic modeling for the catalytic cracking of tires pyrolysis oil. *Fuel* **2022**, *309*, 122055. [CrossRef]
20. Cerqueira, H.S.; Magnoux, P.; Martin, D.; Guisnet, M. Effect of contact time on the nature and location of coke during methylcyclohexane transformation over a USHY zeolite. *Stud. Surf. Sci. Catal.* **1999**, *126*, 105–112.
21. Alkhlel, A.; de Lasa, H. Catalyst/feedstock ratio effect on FCC using different catalysts samples. *Catalysts* **2019**, *9*, 542. [CrossRef]
22. Bartholomew, C.H. Mechanisms of catalyst deactivation. *Appl. Catal. A General* **2001**, *212*, 17–60. [CrossRef]
23. Liao, Y.; Liu, T.; Du, X.; Gao, X. Distribution of Iron on FCC Catalyst and Its Effect on Catalyst Performance. *Front. Chem.* **2021**, *9*, 640413. [CrossRef] [PubMed]
24. Lipin, P.V.; Doronin, V.P.; Gulyaeva, T.I. Conversion of higher n-alkanes under deep catalytic cracking conditions. *Petrol. Chem.* **2010**, *50*, 362–367. [CrossRef]
25. Gayubo, A.G.; Llorens, F.J.; Cepeda, E.A.; Olazar, M.; Bilbao, J. Kinetic modelling for selective deactivation in the skeletal isomerization of n-butenes. *Chem. Eng. Sci.* **1997**, *52*, 2829–2835. [CrossRef]
26. Oudar, J.; Wise, H. *Deactivation and Poisoning of Catalysts*; Marcel Dekker: New York, NY, USA, 1985; Volume 344.
27. Guisnet, M.; Magnoux, P.; Martin, D. Roles of acidity and pore structure in the deactivation of zeolites by carbonaceous deposits. *Stud. Surf. Sci. Catal.* **1997**, *111*, 1–19. [CrossRef]
28. Guisnet, M.; Magnoux, P. Coking and deactivation of zeolites: Influence of the Pore Structure Author links open overlay panel. *Appl. Catal.* **1989**, *54*, 1–27. [CrossRef]
29. Nazarova, G.Y.; Ivashkina, E.N.; Ivanchina, E.D.; Vosmerikov, A.V.; Vosmerikova, L.N.; Antonov, A.V. A Model of Catalytic Cracking: Product Distribution and Catalyst Deactivation Depending on Saturates, Aromatics and Resins Content in Feed. *Catalysts* **2021**, *11*, 701. [CrossRef]
30. Chuzlov, V.; Nazarova, G.; Ivanchina, E.; Ivashkina, E.; Dolganova, I.; Solopova, A. Increasing the economic efficiency of gasoline production: Reducing the quality giveaway and simulation of catalytic cracking and compounding. *Fuel Proc. Technol.* **2019**, *196*, 106139. [CrossRef]
31. Ivanchina, E.; Ivashkina, E.; Nazarova, G. Mathematical modelling of catalytic cracking riser reactor. *Chem. Eng. J.* **2017**, *329*, 262–274. [CrossRef]
32. Nazarova, G.; Ivashkina, E.; Ivanchina, E.; Oreshina, A. Modeling of the catalytic cracking: Catalyst deactivation by coke and heavy metals. *Fuel Proc. Technol.* **2020**, *200*, 12. [CrossRef]